Three-Dimensional Structure of the S4–S5 Segment of the *Shaker* Potassium Channel

Oliver Ohlenschläger,[†] Hironobu Hojo,[‡] Ramadurai Ramachandran,[†] Matthias Görlach,[†] and Parvez I. Haris*
*De Montfort University, The Gateway, Leicester LE1 9BH, United Kingdom, [†]Institut für Molekulare Biotechnologie, Centre for Design and Structure in Biology, D-07708 Jena, Germany, and [‡]Department of Industrial Chemistry, Tokai University, Hiratsuka-shi, Kanagawa 259-1292, Japan

ABSTRACT The propagation of action potentials during neuronal signal transduction in phospholipid membranes is mediated by ion channels, a diverse group of membrane proteins. The S4–S5 linker peptide (S4–S5), that connects the S4 and S5 transmembrane segments of voltage-gated potassium channels is an important region of the *Shaker* ion-channel protein. Despite its importance, very little is known about its structure. Here we provide evidence for an amphipathic α-helical conformation of a synthetic S4–S5 peptide of the voltage-gated *Drosophila melanogaster Shaker* potassium channel in water/trifluoroethanol and in aqueous phospholipid micelles. The three-dimensional solution structures of the S4–S5 peptide were obtained by high-resolution nuclear magnetic resonance spectroscopy and distance-geometry/simulated-annealing calculations. The detailed structural features are discussed with respect to model studies and available mutagenesis data on the mechanism and selectivity of the potassium channel.

INTRODUCTION

Neuronal signal transduction is based on the formation and action of ion channels. Potassium (K^+) channels contribute to the generation and propagation of the action potentials. Knowledge about the membrane proteins forming these channels and their three-dimensional fold in phospholipid membranes is essential to understand the mechanism of action and their selectivity. K^+ channels are a large and diverse group of proteins that occur in most membranes of excitable and inexcitable cells. The crystal-structure determination of a K^+ ion channel from *Streptomyces lividans* (Doyle et al., 1998) is a major breakthrough in the understanding of ion-channel structure. This channel exhibits sequence similarities to other K^+ channels, however it has no segments analogous to the S1–S4 segments found in the much larger *Drosophila melanogaster Shaker* voltage-gated potassium channel. These voltage-gated K^+ channels are assumed to be formed by the assembly of four polypeptide monomers of ~70 kD each (Pongs, 1992). In the absence of high-resolution structures, various theoretical models have been proposed for the structural organization of voltage-gated K^+ channels (Durell et al., 1998; Moczydlowski, 1998; Sansom et al., 2000). According to these models, and based on amino-acid sequence analysis, the structure of the *Shaker* K^+ channel is suggested to consist of six transmembrane helices (S1–S6) and a hairpin structure for the ion-selective pore H5 (P) region. The ion-selective H5 segment is thought to span only the outer portion of the transmembrane region. The rest of the pore should be formed primarily by the S4–S5 linker (L45) and adopt a helical conformation (Durell et al., 1998), and by the C-terminal half of the S6 segment (Liu et al., 1997; Lopez et al., 1994). The S4 segment is the primary voltage sensor for activation gating and moves outwardly during channel activation (Larson et al., 1996; Yang et al., 1996). Durell et al. (1998) suggest that the S4–S5 and S4 segment should be considered as one transmembrane segment because, in the open conformation of the channel, S4 spans only the outer portion of the transmembrane region, whereas S4–S5 spans the inner portion.

Although the voltage-gating mechanism is quite well understood by a combination of molecular modeling, molecular biology, and electrophysiological analysis, there is still a lack of hard structural data from biophysical studies (Clapham, 1999) and structural details are known only for parts of the whole channel ensemble, e.g., the tetramerization domain (Kreusch et al., 1998) and the ball peptides (Wissman et al., 1999; Antz et al., 1997, 1999). Because voltage-gated K^+ channels are not available in large quantities for biophysical analysis, chemical synthesis of peptides corresponding to domains of these ion channels provide an alternative means for the investigation of structure, orientation, and function of selected regions of these proteins. Structural studies of ion-channel peptides has become increasingly popular in recent years (for reviews see Montal, 1995; Cafiso, 1999), and studies have been reported on synthetic peptides corresponding to the proposed ion-selective pore (Haris et al., 1994a), the voltage-gated sensor (Haris et al., 1994b), and the ball peptide (Antz et al., 1997) of voltage-gated K^+ channels. This approach has been successfully utilized in determining conformational behavior of peptide fragments of proteins in aqueous solution and its relevance to the initial steps of protein folding (Dyson and Wright, 1993). The potential of extending this approach toward understanding membrane-protein folding is promis-

Submitted July 19, 2001 and accepted for publication February 8, 2002.
Dedicated to the memory of Professor Dennis Chapman, FRS.
Address reprint requests to Parvez I. Haris, De Montfort University, The Gateway, Leicester LE1 9BH, U.K. Tel.: +44-116-250-6306; Fax: +44-116-257-7287; E-mail: pharis@dmu.ac.uk.

0006-3495/02/06/2995/08 $2.00

ing, as has been demonstrated with bacteriorhodopsin (for a review see Popot, 1993). Nuclear magnetic resonance (NMR) spectroscopy has been used for unraveling the structural details of peptide fragments corresponding to regions of voltage-gated ion-channels (Doak et al., 1996; Antz et al., 1997; Shindo et al., 2001). These studies suggest that peptide fragments may show similar conformations as in the native protein. Additionally, unlike structural studies of large biomacromolecules (Ohlenschläger et al., 1998; Stoldt et al., 1999), a structural characterization of small peptides and smaller, yet important fragments of a larger protein can be carried out without the use of isotope-labeled samples (Shindo et al., 2001; Mulvey et al., 1989).

The present study contributes the NMR structure of the full S4–S5 fragment of the *Shaker* voltage-gated K^+ channel in aqueous trifluoroethanol (TFE) solution and in aqueous phospholipid micelles. S4–S5 has been suggested to be an important region of the *Shaker* channel protein and has been suggested to be part of the voltage sensor and part of the ion-channel pore (Isacoff et al., 1991; McCormack et al., 1991; Holmgren et al., 1996; Durell et al., 1998). It was not possible to compare our NMR structural data with the x-ray crystal structure of the bacterial potassium channel from *Streptomyces lividans* (Doyle et al., 1998), because this channel protein is not voltage dependent and does not contain the S4–S5 segment. Therefore, the results were compared to the model of the *Shaker* channel reported by Durell et al. (1998). According to this modeling study, S4–S5 has been suggested to change its conformation upon channel closing, and it has also been predicted to form an α-helix (Holmgren et al., 1996) and possibly a "leucine-zipper" type structure as suggested by McCormack et al. (1991).

MATERIALS AND METHODS

The primary structure of the peptide fragment of the *D. melanogaster Shaker* K^+ channel S4–S5 is HSKGLQILGRTLKASMRELG. Boc-amino acid derivatives and methylbenzhydrylamine resin were purchased from Peptide Institute Inc. (Osaka, Japan). Peptide synthesis was carried out on an methylbenzhydrylamine resin using a peptide synthesizer 430A (Applied Biosystems Inc., Foster City, CA) using the 0.5-mmol scale double-coupling protocol of the benzotriazole active ester method of the system software version 1.40 NMP/HOBt t-Boc. End capping by acetic anhydride was performed after each amino-acid introduction reaction. The protected peptide resin was treated with anhydrous HF containing 10% anisole at 0° C for 1.5 h and the crude peptide released was purified by high performance liquid chromatography. The purity of the peptide was confirmed by analytical high performance liquid chromatography, amino acid analysis, and matrix-assisted laser desorption/ionization mass spectrometry. The micelle samples were prepared by codissolving the peptide with deuterated dodecylphosphocholine (Avanti Polar Lipids Inc., Alabaster, AL) in H_2O at a 1:60 molar ratio and drying in a Speedvac lyophilizer. After dissolution in water, the pH was adjusted with HCl to 4.7 and 9% D_2O (v/v) was added. 2,2,2-Trifluoroethanol-D3 (D, 99%; TFE) and D_2O was purchased from Cambridge Isotopes Laboratories (Andover, MA). The TFE samples were prepared with a TFE: H_2O ratio of 80:20 with 9% D_2O at pH 2.7. For testing of the structural integrity in water, a sample was prepared with 93% H_2O/7% D_2O. All NMR samples had concentrations of 2 mM. The NMR experiments were performed at the 600- or 750-MHz Varian^{UNITY}*INOVA* spectrometer of the Center for Design and Structure in Biology at a temperature of 313 K for the lipid micelle sample, whereas the experiments in TFE were run at 300 K. Two-dimensional (2D) spectra were collected with quadrature detection by the States–Haberkorn (States et al., 1982) method, processed with the Varian Software VNMR Version 5.2 and analyzed with the program XEASY (Bartels et al., 1995). Chemical shifts were referenced either to the residual methylene resonance of CF_3CD_2OH at 3.88 ppm or the water resonance. Spin system and sequential assignments were achieved by 2D homonuclear double quantum-filtered correlation spectroscopy (Piantini et al., 1982), total correlation spectroscopy (TOCSY) (Bax and Davies, 1985) and nuclear Overhauser and exchange spectroscopy (NOESY) (Jeener et al., 1979; Kumar et al., 1980) experiments. The TOCSY experiments for the TFE sample were performed with mixing times of 60 and 100 ms, the 2D NOESY spectra with 60- and 200-ms mixing time. For S4–S5 in micelles, a TOCSY mixing time of 80 ms and NOESY mixing times of 80 and 200 ms were used. The H/D exchange was followed by a series of one-dimensional NMR experiments in time intervals of 5, 10, 15, 20, and 30 min after addition of D_2O to a lyophilized sample of S4–S5 in micelles. Distance constraints were derived from the 60- or 80-ms NOESY spectra, respectively. Integrals were transformed into distance constraints with the program CALIBA (Güntert et al., 1991). The distance constraints were subjected to a local conformational analysis with the FOUND algorithm (Güntert et al., 1998). The distance-geometry/simulated-annealing calculations were performed with the program DYANA (Güntert et al., 1997) on Silicon Graphics workstations. For the energy minimization, the program OPAL (Luginbühl et al., 1996) utilizing the AMBER4.1 force field (Pearlman et al., 1995) was used. Figures were generated with the program MOLMOL (Koradi et al., 1996).

RESULTS AND DISCUSSION

The S4–S5 segment has been the subject of several mutagenesis, electrophysiological, and molecular modeling studies (Isacoff et al., 1991; McCormack et al., 1991; Holmgren et al., 1996; Durell et al., 1998). However, what has been missing is hard structural data that can be used to rationalize this wealth of mainly functional data. Here we have used NMR spectroscopy to characterize the conformation in a phospholipid membrane system and in TFE and aqueous solution. Although TFE or phospholipid membranes may not directly mimic the in vivo conditions encountered by the peptide fragment in native ion channels, they are widely used as good model systems for gaining insights into factors governing folding of membrane proteins.

The spin system assignment in TFE and in the micellar solution was carried out following the conventional approach as introduced by Wüthrich (1986) utilizing data from double quantum-filtered correlation spectroscopy and TOCSY spectra. The NOESY spectra (see Fig. 1 *A* for the micelle sample) were analyzed to establish the sequential assignment. Based on the complete resonance assignment (Table 1, 2), the chemical shifts of the H^α protons provide information about secondary structure elements following the chemical shift index (CSI) method by Wishart et al. (1992). Interestingly, although, in TFE environment, the CSI of the H^α atoms of S4–S5/TFE clearly predicts an α-helical conformation between Gly-9 and Glu-18. No ev-

TABLE 1 Chemical shift values of L45 in micelles at 40°C

Residue	H^N	H^α	H^β	H^γ	H^δ	H^ε
His-1 (378)	8.72	4.86	3.41 3.23		7.42	8.71
Ser-2 (379)	8.62	4.47	4.12 4.02			
Lys-3 (380)	8.66	4.33	2.00 2.00	1.64 1.58	1.84 1.84	3.11 3.11
Gly-4 (381)	8.79	3.98 3.92				
Leu-5 (382)	8.21	4.24	1.94 1.72	1.88	1.08 1.00	
Gln-6 (383)	8.22	4.23	2.36 2.31	2.64 2.46		7.62 6.93
Ile-7 (384)	8.21	3.95	2.10	1.84 1.34 1.05	1.00	
Leu-8 (385)	8.40	4.18	1.90 1.90	1.83	1.03 1.00	
Gly-9 (386)	8.75	4.03 3.80				
Arg-10 (387)	8.23	4.24	2.11 2.11	1.97 1.85	3.33 3.33	7.53
Thr-11 (388)	8.25	4.17	4.42	1.34		
Leu-12 (389)	8.59	4.21	1.97 1.72	1.92	1.00 0.98	
Lys-13 (390)	8.27	4.09	2.04 2.01	1.69 1.55	1.83 1.83	3.06 3.06
Ala-14 (391)	8.01	4.31	1.66 1.66			
Ser-15 (392)	8.16	4.42	4.10 3.97			
Met-16 (393)	8.15	4.38	2.28 2.24	2.81 2.68		
Arg-17 (394)	7.98	4.24	2.07 2.07	1.88 1.79	3.36 3.36	7.51
Glu-18 (395)	8.07	4.36	2.29 2.21	2.53 2.53		
Leu-19 (396)	7.93	4.37	1.92 1.73	1.91	1.05 1.02	
Gly-20 (397)	8.10	4.03 3.97				

idence for a helical folding could be obtained from the chemical-shift analysis of the peptide in micellar solution (Fig. 1 *B*). The exchange of the labile protons of S4–S5 in micelles revealed a fast exchange behavior of all amide protons. Nevertheless, the nuclear Overhauser enhancement (NOE) pattern given in Fig. 1 *B* and the results of the structure calculations indicate clearly the presence of an α-helix under the micellar conditions as well. This disagreement between observation and CSI prediction suggests that the CSI of H^α protons may not be fully applicable under this solution condition. A further indication for an α-helical conformation spanning the whole peptide sequence were the $^3J_{HNH\alpha}$ coupling constants for S4–S5 in micelles that were found to be lower than 6 Hz for residues 2, 3, 5, 8, 12–14, 17, and 19.

For S4–S5 in TFE (Fig. 2), a total of 423 NOE cross-peaks in the NOESY with 60-ms mixing time amounted in 274 meaningful distance constraints. Structure calculations resulted in a mean target function of 0.14 Å^2 for the 20 best conformers. No van-der-Waals and upper-limit constraint violations were observed after energy minimization that resulted in a mean energy of -238 kcal mol^{-1}. The structures were superimposed with an rmsd to the mean structure of 0.63 $\pm$ 0.15 Å for the backbone and 1.31 $\pm$ 0.15 Å for the heavy atoms.

TABLE 2 Chemical shift values of L45 in 60% TFE at 27°C

Residue	H^N	H^α	H^β	H^γ	H^δ	H^ε
His-1	8.13	4.70	3.33 3.15		7.26	8.47
Ser-2	8.13	4.45	4.07 3.88			
Lys-3	8.19	4.22	1.89 1.89	1.56 1.48	1.74 1.74	2.99 2.99
Gly-4	8.24	3.88 3.84				
Leu-5	7.66	4.22	1.80 1.64	1.74	0.96 0.91	
Gln-6	7.98	4.11	2.29 2.20	2.54 2.43		
Ile-7	7.92	3.81	2.02	1.73 1.73 1.19	0.88	
Leu-8	8.29	4.12	1.90 1.63	1.81	0.91 0.89	
Gly-9	8.48	3.90 3.81				
Arg-10	7.98	4.10	2.00 2.00	1.90 1.74	3.18 3.18	7.14
Thr-11	8.10	4.00	4.45	1.28		
Leu-12	8.61	4.13	1.83 1.75	1.68	0.94 0.91	
Lys-13	8.05	4.05	1.97 1.92	1.65 1.48	1.71 1.71	2.98 2.98
Ala-14	8.17	4.16	1.56 1.56			
Ser-15	8.10	4.33	4.13 3.98			
Met-16	7.99	4.34	2.21 2.17	2.77 2.60		
Arg-17	7.87	4.18	2.00 1.95	1.74 1.74	3.23 3.21	7.14
Glu-18	8.02	4.27	2.21 2.18	2.55 2.52		
Leu-19	7.85	4.33	1.80 1.65	1.74	0.94 0.90	
Gly-20	7.88	3.93 3.90				

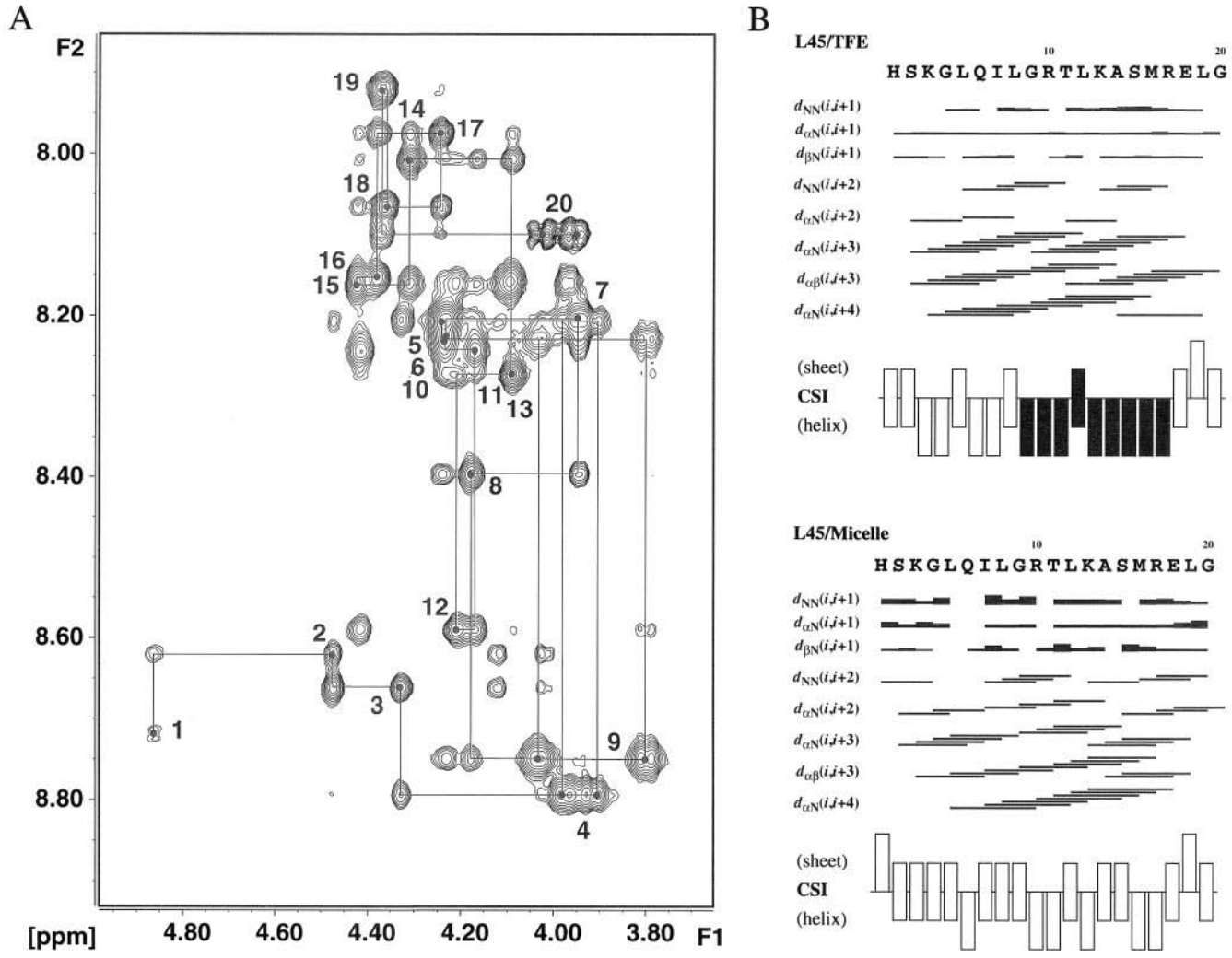

FIGURE 1 (*A*) H^N–H^α region of a 2D NOESY spectrum of S4–S5 in dodecylphosphocholine micelles. The sequential walk and the assignment is indicated. (*B*) NOE connectivities and CSI of S4–S5 in TFE (*upper panel*) and in phospholipid micelles (*lower panel*).

The micellar solution structure (Fig. 3 *A*) was calculated with 354 distance constraints resulting from 382 assigned cross-peaks in a NOESY with 80-ms mixing time and 74 cross-peaks from a NOESY with 200-ms mixing time. These data were submitted to a local conformational analysis resulting in 59 torsion angle constraints (20ϕ, $14\chi_1$, $12\chi_2$, 17ψ). The structure calculations resulted in a mean target function of 0.09 Å^2 for the 20 best conformers that displayed an energy of -262 kcal mol^{-1} after energy minimization. The structures were superimposed with an rmsd to the mean structure of 0.66 ± 0.20 Å for the backbone and 1.19 ± 0.22 Å for the heavy atoms. When only superimposing residues 6–16 (excluding the less-well-defined N- and C-terminal residues 1–5, 19–20) the rmsd to the mean structure drops to 0.08 ± 0.03 Å for the backbone and 0.60 ± 0.08 Å for the heavy atoms.

FIGURE 2 Structure of S4–S5 in TFE. The secondary structure is superimposed by a ribbon diagram on the energy-minimized distance-geometry structure with the lowest target function.

The NMR analysis shows structural deviations when the conformations of the peptide recorded in aqueous TFE and in aqueous phospholipid are compared. The rmsd of the backbone atoms for the residues Lys-3–Arg-17 of the two mean structures is 0.78 Å. In TFE, a stable α-helical segment between residues Thr-11 and Ser-15 is formed, which

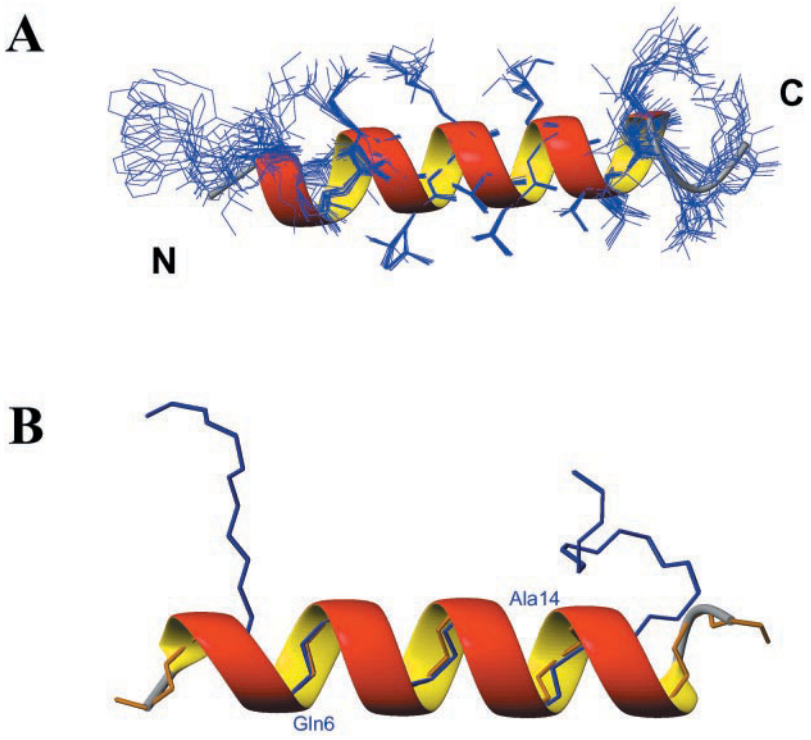

FIGURE 3 (*A*) Structure of S4–S5 in micelles. The 20 best energy-minimized NMR structures are shown. The secondary structure is superimposed by a ribbon diagram of the mean structure. (*B*) Superposition of the backbone of the NMR solution structure of S4–S5 (mean structure; *light*) with the structure of S4–S5 in the open state of the K^+ channel (*dark*) from the modeling studies (Durell et al. 1998).

is separated from a helical N-terminal region between residues Leu-5 and Ile-7 (Fig. 2). The residues Leu-8–Arg-10 exhibit torsion angles characteristic for a bent conformation and thus, although not forming a regular α-helix, lead to an overall straight helical structure.

Under phospholipid micellar conditions, a regular α-helix between residues Lys-3 and Arg-17 is formed. Figure 3 *A* shows a ribbon plot of the S4–S5 structure, indicating also the high definition of the side chain conformations of the hydrophobic residues in the central part of the helix. NMR spectroscopy was also used to determine the presence of structural features of the soluble peptide in a pure aqueous environment (93% H_2O, 7% D_2O). A one-dimensional spectrum (data not shown) indicated chemical shifts in the random coil range of the amino acids (Wüthrich, 1986). The absence of typical NOE cross-peaks in a 2D NOESY spectrum (data not shown) is also consistent with a largely random coil structure of the peptide in aqueous solution. This observation is in agreement with folding predictions by the AGADIR program (Munoz and Serrano, 1994) and indicates that the peptide becomes structured only in the presence of a membrane mimic.

Assuming that the structure determined in the presented fragment approach reflects the conformation in the ion channel, here we have tried to rationalize our results with the available mutagenesis and modeling studies. According to a model proposed by Guy and co-workers (Durell et al., 1998), during channel closure, the S4 and S4–S5 move inward toward the cytoplasm simultaneously, and, as this happens, the S4–S5 helix is suggested to break near its mid-region at the segment 386–388 (Gly-9–Thr-11). This conclusion was based on the low propensity for these residues to form an α-helical conformation. The movement of the S4 segment was recently proven by lanthanide-based resonance energy transfer (Cha et al., 1999). Due to the inward movement of S4–S5, residues 389–391 (Leu-12–Ala-14) should become the N-terminal portion of the S5 helix for the closed conformation (Durell et al., 1998). This mechanism, referred as the "folding zipper," moves the S4–S5 inward by about seven residues and is suggested to happen without eliminating the hydrophobic interactions between leucines, which would explain why mutations of the highly conserved leucines alter the voltage dependency of activation. The differences in helicity observed in our NMR structures are located at residue Arg-10 and thus, directly at the edge of the above mentioned segments 386–388 and 389–391. This stresses the potential of this molecular region for conformational changes under conditions such as opening and closure of the channel and agrees well with the model (Durell et al., 1998).

The model proposed by Durell et al. (1998) additionally suggests that the central ion-permeation pathway is lined by

S4–S5 because it should form an amphipathic α-helix that has a well-conserved hydrophobic face and a poorly conserved hydrophilic face. Assuming S4–S5 is a helix, substituted-cysteine-accessibility method studies (Holmgren et al., 1996) indicated that the highly conserved hydrophobic face forms part of the lining of the inner part of the permeation pore. If this suggestion is taken to be correct, then, according to mutagenesis studies, S4–S5 is likely to be approximately parallel to the axis of the pore, with its rather hydrophobic face oriented toward the pore. Consequently, this requires its more hydrophilic face to be oriented away from the permeation pore, where it could line part of another water-filled pore or cleft. The three-dimensional structure of S4–S5 determined in this study reveals it to adopt an amphipathic structure and fits these suggestions regarding its structural role in the native channel. The determined helix arrangement (Fig. 3 *A*) creates an amphipathicity with residues Gln-6, Arg-10, Lys-13, and Arg-17 on one side and Leu-5, Leu-8, Gly-9, Leu-12, Met-16, and Leu-19 on the hydrophobic side. This conformational feature is supported by a leucine heptad repeat which occurs from the end of S4 through to the first part of S5 observed in many cloned voltage-gated ion-channels (Pongs, 1992). Substitutions of these leucine residues by valines produce large effects on the voltage dependence of conductance curves. Changes in slope were dramatic when L375 and L382 (but not L389) L396 and L403, were substituted by valine. These symmetrical effects were attributed to the general folding model of the *Shaker* channel that locates leucines L375/L382 (Leu-5) and leucines L396 (Leu-19)/L404 into two separate hydrophobic segments S4 and S5, respectively (Pongs, 1992). It has been suggested that the leucines within the heptad repeat are important for stabilizing the conformational changes the *Shaker* channel undergoes during activation.

Shaker K^+ channels respond to membrane depolarization by opening and then rapidly inactivating. This process, referred to as N-type inactivation, has been shown to arise from a tethered blocker mechanism similar to the ball-and-chain model first proposed for the sodium channel inactivation (Armstrong and Bezanilla, 1977). Removal of the ball peptide, which, in the *Shaker* channel, corresponds to the first ~20 residues at the NH_2 terminus (Antz et al., 1997; Hoshi et al., 1990; Zagotta et al., 1990), abolishes the N-type inactivation (Wissmann et al., 1999). Based on site-directed (Isacoff et al., 1991), cysteine-substitution mutagenesis and chemical modification studies (Holmgren et al., 1996), it was shown that the region near alanine 391 (Ala-14) in S4–S5 forms at least part of the receptor for the inactivation gate (Isacoff et al., 1991). Although substitutions at other positions in S4–S5 altered the rates of N-type inactivation, a replacement of glutamate 395 (Glu-18) completely abolished N-type inactivation and led to suggestions that this residue may act as a counter-charge for the positively charged residues of the inactivation ball. Because Glu-395 (Glu-18) is conserved in all voltage-gated K^+ and even a charge-conservative mutation of the Glu-395 with Asp disrupts N-type inactivation (Isacoff et al., 1991), a destabilization of the open state by the mutations is assumed.

Previously, Murrell-Lagnado and Aldrich (1993) reported that increasing the net positive charge of the ball peptide produces an increase in the association rate. This effect has been explained by long-range electrostatic interaction between the peptide and its receptor, which is supported by the chemical modification of 391C (Holmgren et al., 1996). The modification properties of 19 consecutive residues in S4–S5 led to the suggestion that most of the highly reactive residues would be located on one face of the helix, consistent with earlier suggestions about the structure of this region (McCormack et al., 1991; Isacoff et al., 1991) and the results presented here.

The closed-state model by Guy and co-workers (Durell et al., 1998), which resembles a turn around Thr-11, would exhibit NOE correlations between residues 8/15 and 7/18 not observed in our spectra or contradicted by cross-peaks, e.g., between $H^{\alpha 2}_9/H^N_{13}$ or H^{α}_{11}/H^N_{14}. Although the extended N-terminus and the C-terminal turn proposed for the open form (Yang et al., 1996) can be excluded due to the appearance of specific NOE connectivities (e.g., H^{α}_3/H^N_5, H^{α}_3/H^N_6, $H^{\alpha}_3/H^{\gamma 2}_6$, and H^{α}_{14}/H^N_{18}, H^{α}_{15}/H^N_{17}, H^{α}_{15}/H^N_{18}, H^{α}_{17}/H^N_{20}, $H^{\alpha}_{13}/H^{\gamma 2}_{16}$), the extent of similarity between this open-state model and the NMR structure in micelles is significant. From Fig. 3 *B*, it is evident that the helical structures virtually overlap in the region Gln-6 to Ala-14 with an rmsd of 0.42 Å when comparing the backbone atoms. Instead, the TFE structure displays an rmsd of 0.96 Å, indicating the conformational differences in the two solution environments. The open conformation should correspond to the primary conformation of the protein in the endoplasmic reticulum, where there is little or no voltage across the membrane. In this regard, the isolated S4–S5 peptide fragment that we have studied in micellar conditions resembles the structure encountered in the open state of the channel. The model of the ion-selective pore structure proposed by Guy and co-workers (Durell et al., 1998) has been subsequently proven to be remarkably similar to the homologs region of a bacterial K^+ channel (Doyle et al., 1998). The similarity between the structure of the S4–S5 determined using NMR spectroscopy and that modeled by Durell et al., (1998) stresses the value of both molecular modeling and use of isolated peptides for developing a structural model of potassium channels.

Coordinates

The coordinates for the S4–S5 structure in TFE and in aqueous phospholipid micelles have been deposited in the Protein Data Bank (accession codes 1HO7 and 1HO2, respectively).

This work was supported by the Training and Mobility of Researchers Program of the European Commission with the NMR experiments per-

formed at the European Large Scale Facility, Center for Design and Structure in Biology at the Institut für Molekulare Biotechnologie in Jena, Germany (Contract No. ERB FMGE CT98 0121).

We want to thank Dr. H. Robert Guy, National Institutes of Health, Bethesda, MD for providing coordinate sets of his latest ion channel models.

REFERENCES

Antz, C., M. Geyer, B. Fakler, M. K. Schott, H. R. Guy, R., Frank, J. P. Ruppersberg, and H. R. Kalbitzer. 1997. NMR structure of inactivation gates from mammalian voltage-dependent potassium channels. *Nature.* 385:272–275.

Antz, C., T. Bauer, H. Kalbacher, R. Frank, M. Covarrubias, H. R. Kalbitzer, J. P. Ruppersberg, T. Baukrowitz, and B. Fakler. 1999. Control of K^+ channel gating by protein phosphorylation: structural switches of the inactivation gate. *Nature Struct. Biol.* 6:146–150.

Armstrong, C. M., and F. Bezanilla. 1977. Inactivation of the sodium channel. II. Gating current experiments. *J. Gen. Physiol.* 70:567–590.

Bartels, C., T. Xia, M. Billeter, P. Güntert, and K. Wüthrich. 1995. The program XEASY for computer-supported NMR spectral analysis of biological macromolecules. *J. Biomol. NMR.* 6:1–10.

Bax, A., and D. G. Davis. 1985. MLEV-17-based two-dimensional homonuclear magnetization transfer spectroscopy. *J. Magn. Reson.* 65:355–360.

Cafiso, D. S. 1999. Interaction of natural and model peptides with membranes. *Curr. Top. Membr.* 48:197–228.

Cha, A., G. E. Snyder, P. R. Selvin, and F. Bezanilla. 1999. Atomic scale movement of the voltage-sensing region in a potassium channel measured via spectroscopy. *Nature.* 402:809–813.

Clapham, D. E. 1999. More pieces of the K^+ ion channel puzzle. *Nature Struct. Biol.* 6:807–810.

Doak, D. G., D. Mulvey, K. Kawaguchi, J. Villalain, and I. D. Campbell. 1996. Structural studies of synthetic peptides dissected from the voltage-gated sodium channel. *J. Mol. Biol.* 258:672–687.

Doyle, D. A., J. M. Cabral, R. A. Pfuetzner, A. Kuo, J. M. Gulbis, S. L. Cohen, B. T. Chait, and R. MacKinnon. 1998. The structure of the potassium channel: molecular basis of K^+ conduction and selectivity. *Science.* 280:69–77.

Durell, S. R., Y. Hao, and H. R. Guy. 1998. Structural models of the transmembrane region of voltage-gated and other K^+ channels in open, closed, and inactivated conformations. *J. Struct. Biol.* 121:263–284.

Dyson, H. J., and P. E. Wright. 1993. Peptide conformation and protein folding. *Curr. Opin. Struc. Biol.* 3:60–65.

Güntert, P., W. Braun, and K. Wüthrich. 1991. Efficient computation of three-dimensional protein structures in solution from nuclear magnetic resonance data using the program DIANA and the supporting programs CALIBA, HABAS and GLOMSA. *J. Mol. Biol.* 217:517–530.

Güntert, P., M. Billeter, O. Ohlenschläger, L. R. Brown, and K. Wüthrich. 1998. Conformational analysis of protein and nucleic acid fragments with the new grid search algorithm FOUND. *J. Biomol. NMR.* 12: 543–548.

Güntert, P., C. Mumenthaler, and K. Wüthrich. 1997. Torsion angle dynamics for NMR structure calculation with the new program DYANA. *J. Mol. Biol.* 273:283–298.

Haris, P. I., B. Ramesh, M. S. Sansom, I. D. Kerr, K. S. Srai, and D. Chapman. 1994a. Studies of the pore-forming domain of a voltage-gated potassium channel protein. *Protein Eng.* 7:255–262.

Haris, P. I., B. Ramesh, S. Brazier, and D. Chapman. 1994b. The conformational analysis of a synthetic S4 peptide corresponding to a voltage-gated potassium ion channel protein. *FEBS Lett.* 349:371–374.

Holmgren, M., Y. Liu, Y. Xu, and G. Yellen. 1996. On the use of thiol-modifying agents to determine channel topology. *Neuropharmacology.* 35:797–804.

Hoshi, T., W. N. Zagotta, and R. W. Aldrich. 1990. Biophysical and molecular mechanisms of *Shaker* potassium channel inactivation. *Science.* 250:533–538.

Isacoff, E. Y., Y. N. Jan, and L. Y. Jan. 1991. Putative receptor for the cytoplasmic inactivation gate in the *Shaker* K^+ channel. *Nature.* 353: 86–90.

Jeener, J., B. H. Meier, P. Bachmann, and R. R. Ernst. 1979. Investigation of exchange processes by two-dimensional NMR spectroscopy. *J. Chem. Phys.* 71:4546–4553.

Koradi, R., M. Billeter, and K. Wüthrich. 1996. MOLMOL: a program for display and analysis of macromolecular structures. *J. Mol. Graph.* 14: 51–55.

Kreusch, A., P. J. Pfaffinger, C. F. Stevens, and S. Choe. 1998. Crystal structure of the tetramerization domain of the *Shaker* potassium channel. *Nature.* 392:945–948.

Kumar, A., R. R. Ernst, and K. Wüthrich. 1980. A two-dimension nuclear Overhauser enhancement (2D NOE) experiment for the elucidation of complete proton–proton cross-relaxation networks in biological macromolecules. *Biochem. Biophys. Res. Comm.* 95:1–6.

Larson, H. P., O. S. Baker, D. S. Dhillon, and E. Y. Isacoff. 1996. Transmembrane movement of the *Shaker* K^+ channel S4. *Neuron.* 16:387–397.

Liu, Y., M. Holmgren, M. E. Jurman, and G. Yellen. 1997. Gated access to the pore of a voltage-dependent K^+ channel. *Neuron.* 19:175–184.

Lopez, G. A., Y. N. Jan, and L. Y. Jan. 1994. Evidence that the S6 segment of the *Shaker* voltage-gated K^+ channel comprises part of the pore. *Nature.* 367:179–182.

Luginbühl, P., P. Güntert, M. Billeter, and K. Wüthrich. 1996. The new program OPAL for molecular dynamics simulations and energy refinements of biological macromolecules. *J. Biomol. NMR.* 8:136–148.

McCormack, K., M. A. Tanouye, L. E. Iverson, J. W. Lin, M. Ramaswami, T. McCormack, J. T. Campanelli, M. K. Mathew, and B. Rudy. 1991. A role for hydrophobic residues in the voltage-dependent gating of *Shaker* K^+ channels. *Proc. Natl. Acad. Sci. U.S.A.* 88:2931–2935.

Moczydlowski, E. 1998. Chemical basis for alkali cation selectivity in potassium-channel proteins. *Chem. Biol.* 5:R291–R301.

Montal, M. 1995. Protein folds in channel structure. *Curr. Opin. Struc. Biol.* 5:501–506.

Mulvey, D., G. F. King, R. M. Cooke, D. G. Doak, T. S. Harvey, and I. D. Campbell. 1989. High resolution 1H NMR study of the solution structure of the S4 segment of the sodium channel protein. *FEBS Lett.* 257:113–117.

Munoz, V., and L. Serrano. 1994. Elucidating the folding problem of helical peptides using empirical parameters. *Nature Struct. Biol.* 1:399–409.

Murrell-Lagnado, R. D., and R. W. Aldrich. 1993. Interactions of amino terminal domains of *Shaker* K channels with a pore blocking site studied with synthetic peptides. *J. Gen. Physiol.* 102:949–975.

Ohlenschläger, O., R. Ramachandran, K.-H. Gührs, B. Schlott, and L. R. Brown. 1998. Nuclear magnetic resonance solution structure of the plasminogen-activator protein staphylokinase. *Biochemistry.* 37: 10635–10642.

Pearlman, D. A., D. A. Case, J. W. Caldwell, W. S. Ross, T. E. Cheatham, III, D. M. Ferguson, G. L. Seibel, U. Chandra Singh, P. K. Weiner, and P. A. Kollman. 1995. AMBER 4.1. University of California, San Francisco, CA.

Piantini, U., O. W. Sørensen, and R. R. Ernst. 1982. Multiple quantum filters for elucidating NMR coupling networks. *J. Am. Chem. Soc.* 104: 6800–6801.

Pongs, O. 1992. Molecular biology of voltage-dependent potassium channels. *Physiol. Rev.* 72:S69–S88.

Popot, J. L. 1993. Integral membrane protein structure–transmembrane alpha-helices as autonomous folding domains. *Curr. Opin. Struc. Biol.* 3:532–540.

Sansom, M. S. P., I. H. Shrivastava, K. M. Ranatunga, and G. R. Smith. 2000. Simulations of ion channels—watching ions and water move. *Trends Biochem. Sci.* 25:368–374.

Shindo, K., H. Takahashi, K. Shinozaki, K. Kami, K. Anzai, S. Lee, H. Aoyagi, Y. Kirino, and I. Shimada. 2001. Solution structure of micelle-bound H5 peptide (427–452): a primary structure corresponding to the

pore forming region of the voltage dependent potassium channel. *Biochim. Biophys. Acta.* 1545:153–159.

States, D. J., R. A. Haberkorn, and D. J. Ruben. 1982. A two-dimensional nuclear Overhauser experiment with pure absorption phase in four quadrants. *J. Magn. Reson.* 48:286–292.

Stoldt, M., J. Wöhnert, O. Ohlenschläger, M. Görlach, and L. R. Brown. 1999. The NMR structure of the 5S rRNA E-domain/protein L25 complex shows pre-formed and induced recognition. *EMBO J.* 18: 6508–6521.

Wishart, D. S., B. D. Sykes, and F. M. Richards. 1992. The chemical shift index: a fast and simple method for the assignment of protein secondary structure through NMR spectroscopy. *Biochemistry.* 31:1647–1651.

Wissmann, R., T. Baukrowitz, H. Kalbacher, H. R. Kalbitzer, J. P. Ruppersberg, O. Pongs, C. Antz, and B. Fakler. 1999. NMR structure and functional characteristics of the hydrophilic N terminus of the potassium channel beta-subunit Kvbeta1.1. *J. Biol. Chem.* 274:35521–35525.

Wüthrich, K. 1986. NMR of Proteins and Nucleic Acids. Wiley, New York.

Yang, N. B., A. L. George, and R. Horn. 1996. Molecular basis of charge movement in voltage-gated sodium channels. *Neuron.* 16:113–122.

Zagotta, W. N., T. Hoshi, and R. W. Aldrich. 1990. Restoration of inactivation in mutants of *Shaker* potassium channels by a peptide derived from ShB. *Science.* 250:568–571.